atmosphere

Article

Weakened Connection between East China Summer Rainfall and the East Asia-Pacific Teleconnection Pattern

Xiaoxue Yin, Lian-Tong Zhou * and Jingliang Huangfu

Center for Monsoon System Research, Institute of Atmospheric Physics, Chinese Academy of Sciences, Beijing 100029, China; yxx@mail.iap.ac.cn (X.Y.); hfjl@mail.iap.ac.cn (J.H.)
* Correspondence: zlt@mail.iap.ac.cn

Abstract: The interdecadal change in the relationship between the East Asia-Pacific (EAP) teleconnection pattern and rainfall over East China during boreal summer (June–August) was investigated using observation and reanalysis datasets during 1951–2018. As proposed in a previous study, summer rainfall in the Yangtze-Huaihe River (YH-R) valley is below (above) normal when a positive (negative) EAP event occurs. Based on the close relationship with the rainfall anomalies, the EAP teleconnection pattern has been widely used in the prediction of summer rainfall variations in the YH-R valley. However, we found that the rainfall anomalies in the YH-R basin associated with the EAP pattern were weaker and less evident after the late 1980s. This finding indicates a decreased relationship between the EAP pattern and YH-R basin summer rainfall after the late 1980s, and a decrease in the quality and skill of seasonal predictions of YH-R basin summer rainfall related to the EAP pattern. This pronounced weakening in the YH-R summer rainfall-EAP pattern connection is attributed to the northeastward displacement of the Japanese action center of the EAP pattern after the late 1980s, which caused weaker anomalous vertical motion and moisture transportation over the YH-R valley. The present research reveals that the interdecadal expansion in the size of the Indo-Pacific warm pool in the late 1980s is likely responsible for the northeastward shift in the Japanese action center of the EAP teleconnection pattern by modulating anomalous convective activities and the northward propagation of the EAP pattern.

Keywords: East China summer rainfall; East Asia-Pacific pattern; interdecadal shift; Indo-Pacific warm pool

Citation: Yin, X.; Zhou, L.-T.; Huangfu, J. Weakened Connection between East China Summer Rainfall and the East Asia-Pacific Teleconnection Pattern. *Atmosphere* **2021**, *12*, 704. https://doi.org/10.3390/atmos12060704

Academic Editor: Roberto Fraile

Received: 10 May 2021
Accepted: 27 May 2021
Published: 30 May 2021

1. Introduction

Over East China, the summer (June–August (JJA)) rainfall anomaly is an important climate change variable that causes severe droughts and floods [1]. The catastrophic flood that occurred in the Yangtze River valley in the summer of 1998 resulted in immense damage to the local economy, society, and people's lives [2]. Therefore, it is important to improve the understanding of summer rainfall variability over East China, which may contribute to reductions in damage and losses caused by anomalous droughts and floods.

Substantial effort has been devoted to understanding the variations in summer rainfall over East China [3–8]. The East Asia-Pacific (EAP) pattern [3], also known as the Pacific-Japan (PJ) pattern [9], is one of the most important factors that has crucial influences on summer rainfall anomalies in East China, especially in the Yangtze-Huaihe River (YH-R) basin [10–15]. Huang [10] found a close negative relationship between the interannual variations in YH-R valley summer rainfall and the EAP teleconnection pattern. Li et al. [13] revealed the critical impacts of the low-frequency EAP pattern oscillations on persistent, heavy precipitation over the YH-R valley. Extreme rainfall anomalies occur in negative EAP events, such as the major floods in the Yangtze River basin in the summer of 1998 [2]. Based on the close relationship with rainfall anomalies, the EAP teleconnection pattern has been widely used in the prediction of summer rainfall in the YH-R valley over East China [10,13,16].

The EAP pattern, which is characterized by a zonally elongated meridional dipole of anomalous centers, displays negative height anomalies near the Philippines over the tropical western North Pacific (WNP) and positive height anomalies over extratropical East Asia around southern Japan in its normal positive phase [17–20]. This pattern can force a remote seesaw-like relationship between summer rainfall anomalies over the midlatitudes of East Asia, namely, the mei-yu/baiu/changma (Meiyu) band stretching from the YH-R valley to southern Japan and regions over the SCS and Philippine Sea [4,21–24]. Concurrent with the positive EAP teleconnection phase, a pronounced anticyclonic circulation anomaly appears south of Japan, and a notable cyclonic circulation anomaly appears near the Philippines over the WNP, resulting in an eastward retreat and northward shift in the western Pacific subtropical high (WPSH) [6,25], which leads to weaker moisture transportation into the midlatitudes of East Asia due to the eastward-shifted southwesterly wind along the western boundary of the WPSH; consequently, this lack of moisture reduces the summer rainfall in the YH-R valley over East China [26,27]. Opposite results occur in the negative EAP teleconnection phase.

The EAP teleconnection pattern is considered to be a northward-propagating Rossby wave train triggered by anomalous heating related to the convective activity anomaly near the Philippines [28–30], which is most efficiently controlled by the thermal state of the Indo-Pacific warm pool (IPWP) [9,14,31]. When the warm pool is in a warm (cold) state, the convective activity is above (below) normal around the Philippines [10,31]. This anomalous heating (cooling) source induces a positive (negative) phase of the EAP pattern via quasi-stationary planetary waves [3], resulting in the out-of-phase rainfall relationship between the midlatitudes of East Asia and the tropical WNP mentioned above. Several studies noted a remarkable eastward extension of warming in the sea surface temperature (SST) over the warm pool in the 1980s [32,33]. Accordingly, the convective activity over the Philippines was enhanced, which could result in significant impacts on East Asia summer climate variations [34–39]. Zhou [32] demonstrated the interdecadal shift in the size of the IPWP in approximately 1986, and suggested that a large warm pool contributed to the increased rainfall in Southeast China after 1986 by inducing stronger surface latent heat fluxes and water vapor amounts. Yin et al. [33] examined and documented the remarkable eastward extension of SST warming over the IPWP in the late 1980s and its impacts on the intensity of the South China Sea summer monsoon. However, the possible influence of this SST extension over the warm pool on the EAP pattern remains unexplored.

The stability of the relationship between the impact factors and rainfall, often displaying interdecadal changes [40], is a fundamental issue in climate variability research. A question to be addressed in the present study is whether the interannual relationship between the EAP pattern, a key forecast index for the climate variability over East China, and the YH-R summer rainfall has experienced any interdecadal changes during the last half century. Another interesting issue to be considered is whether the interdecadal extension in the size of the IPWP plays a role in the stability of the EAP-rainfall relationship. The rest of the paper is organized as follows. Section 2 describes the datasets and methods. Section 3 presents the decadal change in the relationship between summer rainfall and the EAP pattern. Section 4 shows the change in the structure of the EAP pattern and the possible impacts from the interdecadal extension in the IPWP size. Section 5 summarizes the main results and provides further discussion.

2. Data and Methods

The datasets used in this study are described as follows. The monthly mean rainfall data were from 160 stations of the Chinese Meteorological Data Center in China for the period of 1951–2018, which meets the standards of the World Meteorological Organization. The National Oceanic and Atmospheric Administration (NOAA) precipitation reconstruction dataset (PREC) was employed with a horizontal resolution of $1.0^\circ \times 1.0^\circ$ and spanning from 1948 to the present [41]. The monthly mean geopotential height and vector winds were provided by the National Centers for Environmental Prediction-National Center for

Atmospheric Research (NCEP/NCAR), with a horizontal resolution of 2.5° × 2.5° from 1948 to present [42]. The vertically integrated moisture was calculated by employing the specific humidity, air temperature, and surface pressure from the NCEP/NCAR reanalysis data from 1000 to 300 hPa. The monthly mean SST was from the NOAA Extended Reconstruction version 3 (ERSST.v3b), and has a resolution of 2.0° × 2.0° and spans the period from 1854 to present [43].

Following Huang [10], the EAP index is defined as follows:

$$I_{EAP} = -0.25Z_s'\left(60^{\circ}N, 125^{\circ}E\right) + 0.50Z_s'\left(40^{\circ}N, 125^{\circ}E\right) - 0.25Z_s'\left(20^{\circ}N, 125^{\circ}E\right) \quad (1)$$

where $Z_s = Zsin45^{\circ}/sin\varphi$ is the standardized JJA 500 hPa height anomaly at a grid point with latitude φ, and $Z' = Z - \overline{Z}$ is the JJA 500 hPa height anomaly. A positive (negative) I_{EAP} indicates a positive (negative) height anomaly over midlatitude East Asia and a negative (positive) height anomaly over eastern Siberia and the tropical WNP. The size of the IPWP is defined as the region with SSTs warmer than the 29 °C isotherm divided by the climatological warm pool region [32,33]. The main statistical methods adopted here were canonical correlation analysis and linear regression analysis. The two-tailed Student's *t* test was used to assess the confidence level of the linear correlation-regression patterns.

3. Results

3.1. Interdecadal Change in the YH-R Summer Rainfall-EAP Connection

To explore the robustness of the summer rainfall–EAP relationship, the correlation between the EAP index and the China station rainfall in JJA was examined, as shown in Figure 1. Correlation coefficients for a sliding 23-year moving window between the summer YH-R rainfall index, defined as the normalized summer rainfall anomalies averaged over the region (28–33° N, 110–123° E), and the EAP index (multiplied by −1.0) display an obvious decrease after the late 1980s (Figure 1a). For the period of the 1970s and 1980s, the correlation coefficients between the YH-R rainfall and the EAP index are approximately 0.60, and significant at the 95% confidence level. They decrease to approximately 0.2 for the period of the 1990s and 2000s. This result indicates that the EAP pattern can only explain approximately 4% of the summer YH-R rainfall variance after the late 1980s compared with the stronger 36% before the late 1980s.Therefore, the weakened EAP–summer YH-R rainfall relationship diminishes the influence of the EAP pattern on the East China summer rainfall after the late 1980s. Notably, this result is not sensitive to the width of the window, and consistent results were obtained based on different window lengths (e.g., 17, 19, and 21 years; figures not shown). In the following, we used high- and low-correlation periods to further investigate the interdecadal change between the EAP pattern and the YH-R summer rainfall. Based on the sliding correlation in Figure 1a, we selected one high-correlation period (1951–1986, hereafter abbreviated as T1) and one low-correlation period (1987–2018, hereafter abbreviated as T2). The correlation coefficient between the EAP index and the YH-R summer rainfall index for T1 is 0.46, significant at the 99% confidence level, whereas the correlation coefficient in T2 is 0.31 and insignificant at the 95% confidence level.

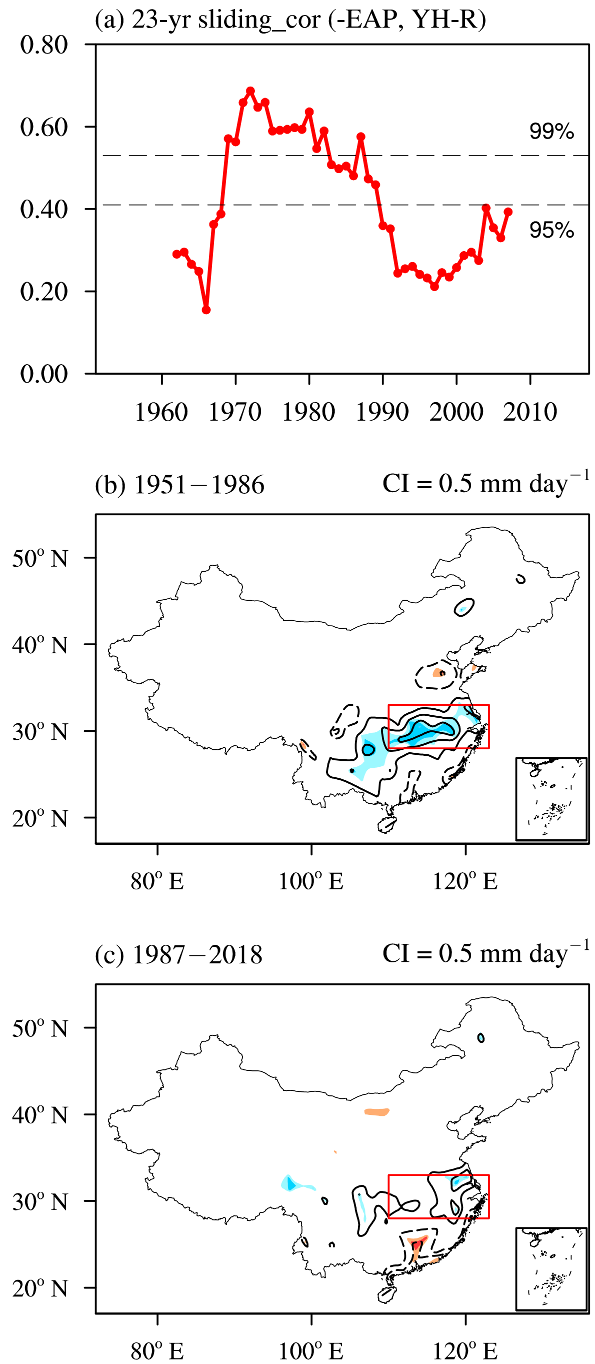

Figure 1. (**a**) Time series of the running correlation with a 23-year window between the EAP index (multiplied by −1.0) and the normalized JJA rainfall anomalies in the Yangtze River and Huaihe River valley (YH-R; 28–33° N, 110–123° E) during 1951–2018. Regression maps of the JJA rainfall anomalies (contour; unit: mm day^{-1}) in China with respect to the EAP index (multiplied by −1.0) during (**b**) 1951–1986 and (**c**) 1987–2018. Positive (negative) values are indicated by solid (dashed) contours with the zero contour omitted. The three orange (blue) shadings from shallow to deep indicate that positive (negative) anomalies are significant at the 90%, 95%, and 99% confidence levels based on a two-tailed Student's t test, respectively. The red boxes in (**b**,**c**) indicate the YH-R basin.

The above interdecadal change is further demonstrated in the spatial distribution of the regressed summer rainfall anomalies over China with respect to the EAP index (Figure 1b,c). The summer rainfall anomalies associated with the EAP pattern before and after the late 1980s show the common feature that a negative EAP pattern is accompanied by positive rainfall anomalies in the YH-R basin, which is consistent with previous studies [44]. However, this positive rainfall sign covers the entire YH-R basin in T1 with a high significance level (Figure 1b) but is much weaker and nonsignificant in T2, covering only the lower reaches of the YH-R basin (Figure 1c). These notable differences in the two subperiods suggest that the EAP teleconnection pattern is closely related to the interannual variations in the summer rainfall anomalies in the YH-R valley before the late 1980s but not in the subsequent period.

The positive rainfall anomalies in the YH-R basin based on the station observations associated with the EAP pattern are part of the Meiyu rainband over midlatitude East Asia, which is often seen in boreal summer [45]. In addition, previous studies reveal an out-of-phase relationship between the summer rainfall anomalies over midlatitude East Asia and the tropical WNP [9,17], which are linked by the EAP pattern. To explore the possible changes in this seesaw relationship between the summer rainfall anomalies over midlatitude East Asia to tropical WNP areas, anomalous rainfall regressed against the EAP index in the two periods based on the gridded rainfall data from the PREC is demonstrated in Figure 2. Generally, the seesaw relationship of summer rainfall anomalies between midlatitude East Asia and the tropical WNP is observed in both periods. However, the region of the positive anomalies over the middle and lower reaches of the YH-R valley during period T2 (Figure 2b) is much smaller than that in period T1 (Figure 2a), indicating that the EAP-related summer rainfall anomalies over the YH-R basin become less evident after the late 1980s, which is consistent with the results obtained in Figure 1. The regions of the anomalous Meiyu band obviously shrink and can only be perceived in South Korea and Japan during T2 (Figure 2b). In addition, the anomalous rainfall over midlatitude East Asia during T2 displays a slight northeastward shift. The domain of the positive rainfall anomalies over midlatitude East Asia displaces northeastward by approximately 2° to 3°, from the East China Sea and south of Japan to South Korea and all of Japan in T2 compared with T1. In addition, negative rainfall anomalies over the tropical WNP are enhanced and expanded slightly northward after the late 1980s. These results confirm the weakening relationship between the YH-R valley summer rainfall anomalies and the EAP pattern, in addition to a northeastward shift in the Meiyu rainband over midlatitude East Asia after the late 1980s.

3.2. Possible Reasons for the Interdecadal Change in the Rainfall–EAP Connection

To understand why the relationship between the YH-R summer rainfall and EAP pattern has decreased, the circulation anomaly distributions related to the EAP index between T1 and T2 are compared. Figure 3a,b demonstrates the anomalies of relative vorticity regressed against the EAP index at 850 hPa, in addition to the wave activity flux in the two subperiods to explore the possible changes in the EAP teleconnection. The atmospheric vertical motion and moisture supply are the two primary factors affecting the precipitation anomalies; thus, the divergence of the horizontal vector wind at 200 hPa and the anomalous moisture transportation integrated from 1000 to 300 hPa were investigated (Figure 3c–f) using the same regression.

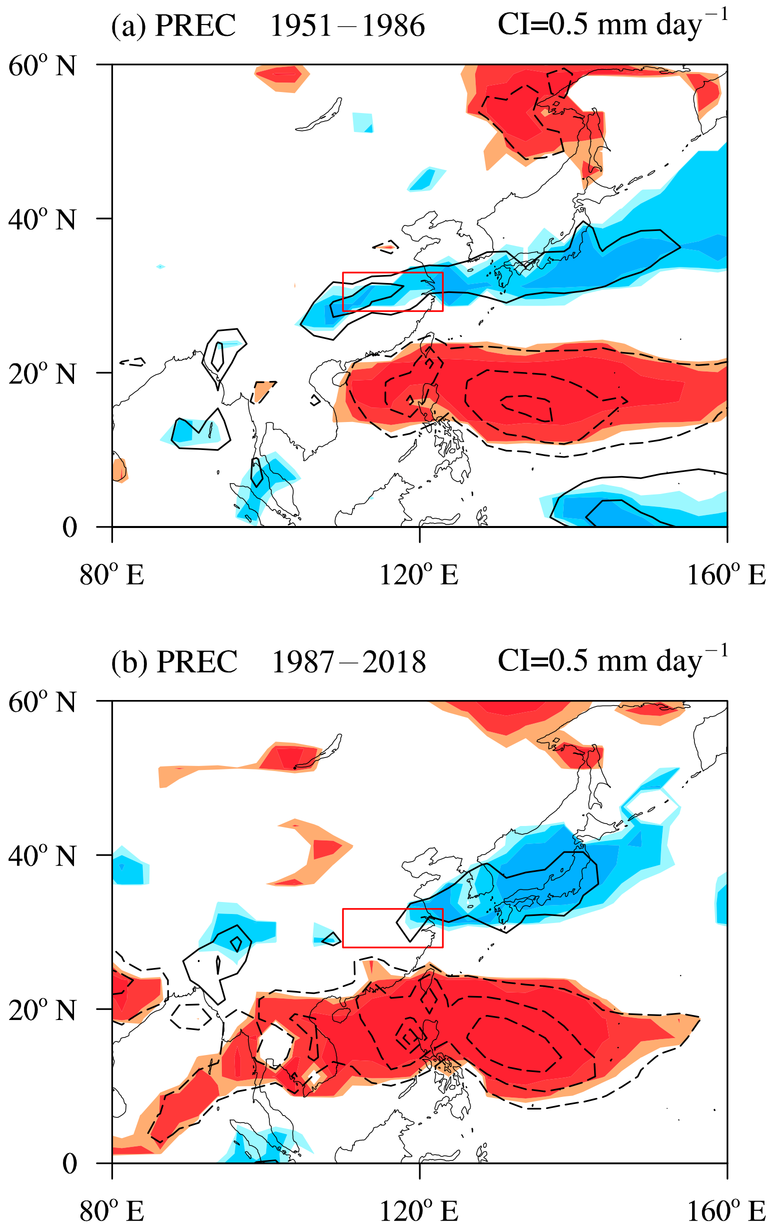

Figure 2. Regression maps of the JJA PREC rainfall (contour; unit: mm day^{-1}) with respect to the normalized EAP index (multiplied by -1.0) for periods (**a**) 1951–1986 and (**b**) 1987–2018. Positive (negative) values are indicated by solid (dashed) contours with the zero contour omitted. The three orange (blue) shadings from shallow to deep indicate that positive (negative) anomalies are significant at the 90%, 95%, and 99% confidence levels based on a two-tailed Student's t test, respectively. The red boxes indicate the YH-R basin.

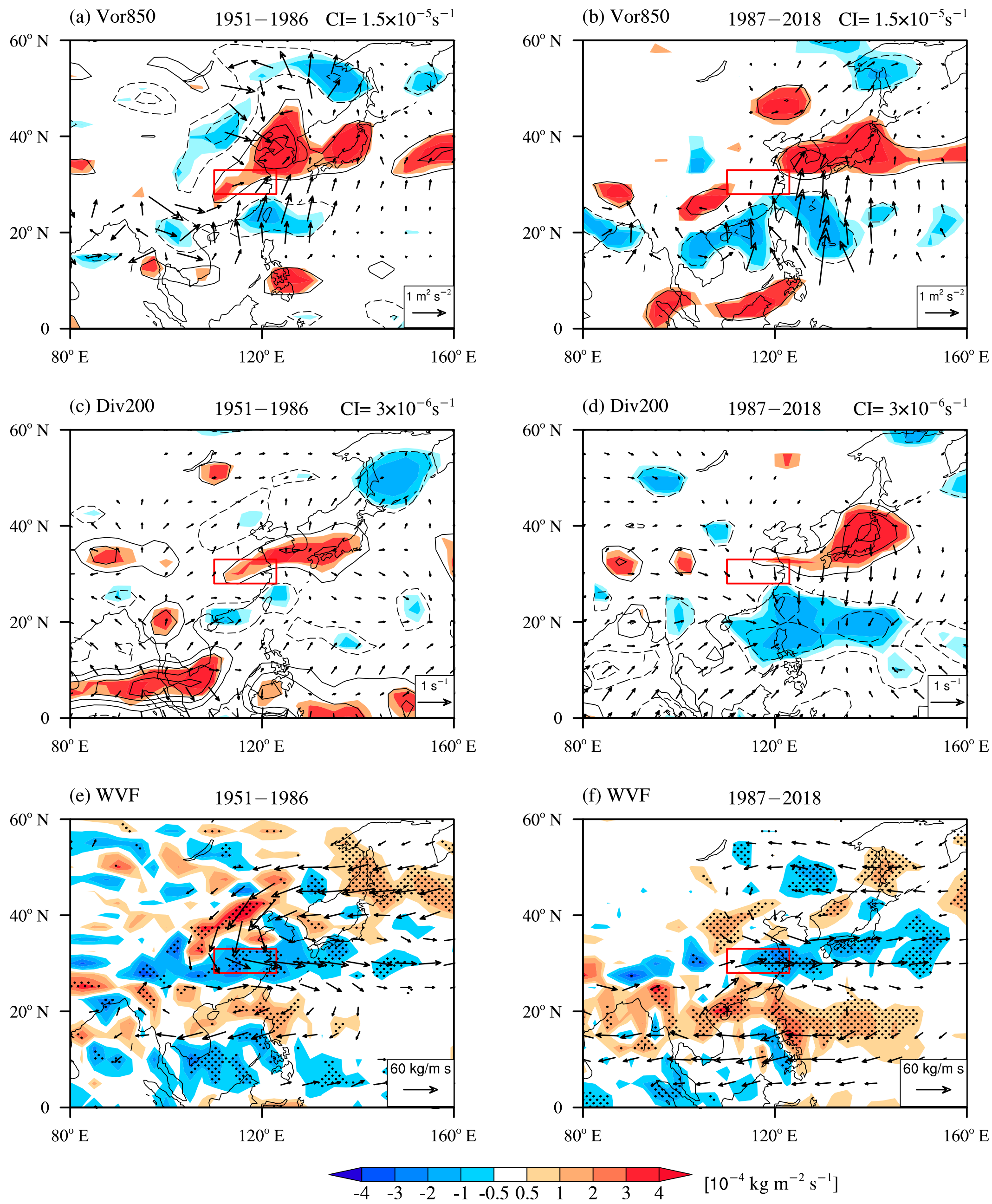

Figure 3. (**a**,**b**) Regression maps of the JJA relative vorticity (contour; unit: s^{-1}) and the associated wave activity flux (vector; unit: $m^2\ s^{-2}$) at 850 hPa with respect to the normalized EAP index (multiplied by -1.0) for 1951–1986 and 1987–2018, respectively. (**c**,**d**) Same as for (**a**,**b**) but for the divergence (contour; unit: s^{-1}) and the divergent wind (vector; m s^{-1}) at 200 hPa. (**e**,**f**) Same as for (**a**,**b**) but for the water vapor flux integration of 1000–300 hPa (vector; unit: kg $m^{-1}\ s^{-1}$) and its divergence (shading; unit: 10^{-4} kg $m^{-2}\ s^{-1}$). In (a–d), positive (negative) values are indicated by solid (dashed) contours with the zero contour omitted. The three orange (blue) shadings from shallow to deep in (**a**–**d**) indicate that positive (negative) anomalies are significant at the 90%, 95%, and 99% confidence levels based on a two-tailed Student's t test, respectively. The dotted regions in (**e**–**f**) indicate the 90% confidence level based on Student's t test. The red boxes indicate the YH-R basin.

Following Kosaka and Nakamura [20], the anomalous summer relative vorticity at 850 hPa was examined (contours; Figure 3a,b); this is usually used to represent the EAP-related circulation. A meridional dipole of zonally elongated centers is observed in the two subperiods, with anticyclonic and cyclonic vorticity anomalies located over the region surrounding the Philippines in the WNP (hereafter referred to as the WNP action center) and the region over Japan in the midlatitudes of East Asia (hereafter referred to as the Japanese action center), respectively. The horizontal wave activity flux [46], which is used to describe the propagation of the Rossby wave train, a result of the EAP pattern, derives from regions around the Philippines and spreads northeastward to the cyclonic vorticity anomalies over the midlatitudes (vectors; Figure 3a,b), which is consistent with previous studies [9]. However, notable differences are also observed between the two subperiods. Clearly, relative to its position in T1, the Japanese action center has a northeastward shift in T2, which is similar to previous research [47]. The positive vorticity anomalies occupy large regions from the mid-lower reaches of the Yangtze River valley to the Korean Peninsula and Japan in the first subperiod. In contrast, these positive anomalies shift northeastward to the Korean Peninsula and Japan in the second subperiod; that is, the significant sign over the Yangtze River valley has disappeared, which might contribute to the weak rainfall anomalies there.

The northeastward displacement of the Japanese action center after the late 1980s can also be detected from the EAP-related atmospheric divergence field (Figure 3c,d) and moisture transportation (Figure 3e,f). Regions over the midlatitudes of East Asia with anomalous upper-tropospheric divergence (Figure 3c,d), which indicate ascending motion anomalies in the lower troposphere, correspond well with regions of positive summer rainfall anomalies (Figure 2) in both subperiods. However, the EAP-related upper-tropospheric divergence patterns are distinctly different between T1 and T2. In T1, a divergent line is seen along the Meiyu band, stretching from the YH-R valley to the area south of Japan (Figure 3c). This divergent sign moves out of the YH-R basin and shifts northeastward to the area east of Japan in T2 (Figure 3d), which is consistent with the weak rainfall anomalies over the YH-R basin shown in Figure 2b. In addition, compared with the results in T1, the upper-tropospheric convergent center over the Philippines has notably enhanced and expanded eastward to the longitude near 140° E in T2. Concurrent with the northeastward shift in the Japanese action center of the EAP pattern after the late 1980s, the associated anomalous water vapor transportation also displays an evident northeastward displacement (Figure 3e,f). In T1, there is greater anomalous moisture flux convergence over the YH-R valley (Figure 3e), which is consistent with the obvious positive rainfall anomalies there (Figure 2a). In contrast, the anomalous moisture flux obviously shrinks to the lower reaches of the Yangtze River basin in T2 (Figure 3f), which clearly has impacts on the rainfall anomalies over the YH-R basin. Moreover, a larger anomalous moisture flux divergence is observed over the tropical WNP regions in T2, corresponding with the suppressed summer rainfall anomalies there (Figure 2b).

Therefore, compared with the period before the late 1980s, the Japanese action center of the EAP pattern has a visible northeastward shift after the late 1980s, which contributes to the weakened YH-R valley rainfall–EAP pattern relationship through evident changes in the anomalous vertical movement and water vapor transport. However, the possible mechanism responsible for the northeastward displacement of the Japanese action center of the EAP pattern is still unclear. As suggested by previous studies [47–49], the variability in the structure of the EAP pattern is related to the shift in the location of the anomalous SST and convective activities. In the following analysis, we attempt to explore why the signal of the Japanese action center of the EAP pattern shifts more northeastward after the late 1980s from the perspective of the interdecadal extension in the size of the IPWP around the late 1980s [32,33].

As defined in the study by Yin et al. [33], the normalized IPWP size index is calculated as the SST region warmer than 29.0 °C divided by the climatological warm pool region, which depicts an obvious increase in the late 1980s (Figure 4). In particular, relative to the area of the warm pool in T1, the eastern and northern boundaries of the warm pool have evidently enlarged eastward and northward by approximately 5° to 20° longitude (Figure 4a). The time series of the IPWP size index (Figure 4b; black line) shows an evident increase in the late 1980s, which indicates an interdecadal extension in the warm pool area. The values of the standardized warm pool size index transfer from below zero to above zero around 1986 (Figure 4b; vertical black line), suggesting a smaller than climatologic warm pool in the former period and a larger than climatologic warm pool in the latter period. This enlargement in the IPWP region includes an increasing trend component and an interdecadal component, which together result in the areal expansion of the IPWP in the late 1980s. Thus, the present study focused on the overall variability in the size of the IPWP to explain the weakened relationship between the EAP teleconnection and the YH-R summer rainfall.

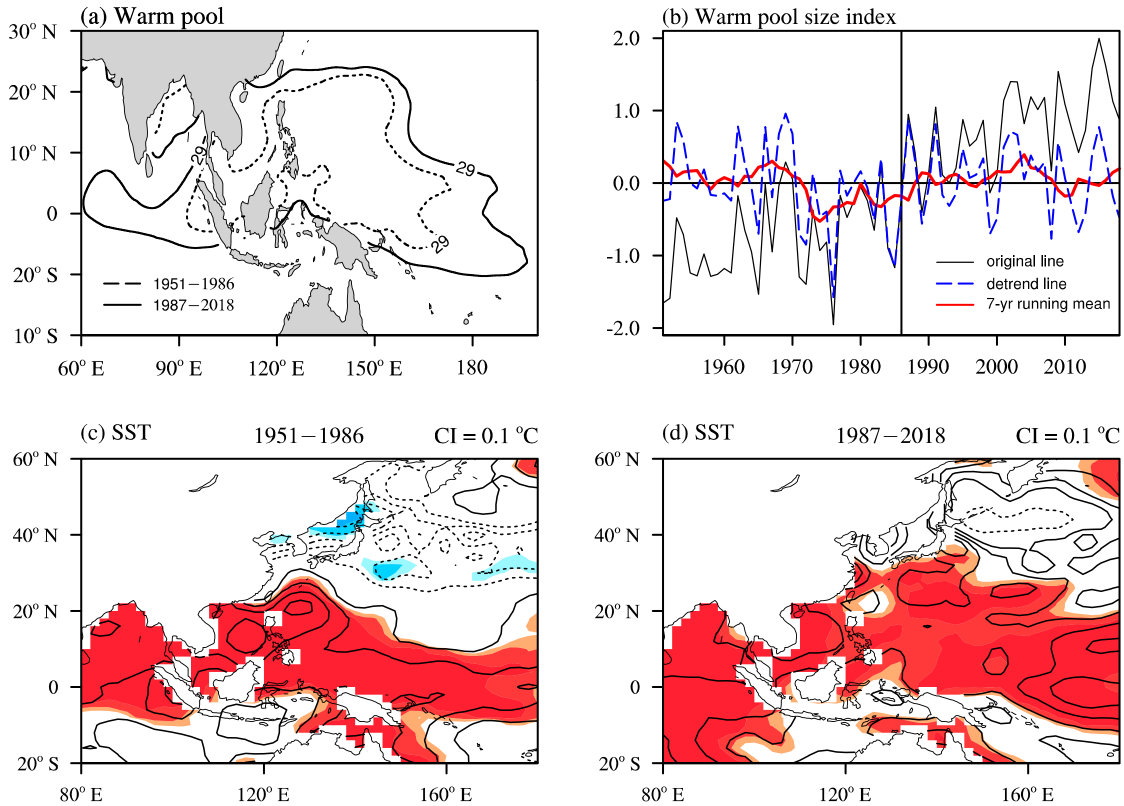

Figure 4. (**a**) Distributions of the JJA 29.0 °C isothermal lines of SST in the Indo-Pacific warm pool (IPWP) during 1951–1986 (dashed line) and 1987–2018 (solid line). (**b**) Time series of the normalized IPWP size index calculated as the region of SST warmer than 29.0 °C divided by the climatological warm pool region in JJA from 1951 to 2018 (black solid curve). The blue dashed curve is the detrended time series, and the red curve is the 9-year running average of the detrended line. (**c**,**d**) Regression maps of SST (contour; unit: °C) with respect to the normalized IPWP index for 1951–1986 and 1987–2018, respectively. Positive (negative) values are indicated by solid (dashed) contours with the zero contour omitted. The three orange (blue) shadings from shallow to deep in (**c**,**d**) indicate that positive (negative) anomalies are significant at the 90%, 95%, and 99% confidence levels based on a two-tailed Student's t test, respectively.

According to the extension of the IPWP area, significant differences in the spatial distribution of the anomalous SSTs (Figure 4c,d) and atmospheric circulations (Figure 5) before and after the late 1980s are detected. During 1951–1986, significant positive SST anomalies are seen in the warm pool area (Figure 4c). A meridional tripole pattern is observed along East Asia and the WNP area in the troposphere (Figure 5a) and high troposphere (not shown), featuring a barotropic structure tilting slightly northward with height [19]. This distribution of the anomalous relative vorticity is similar to that related to the EAP index (Figure 3a). Therefore, this distribution suggests a close connection between the thermal states of the IPWP and the EAP pattern in the former period, which is consistent with previous studies [14,31]. Accordingly, significant moisture flux anomaly convergence is observed over the YH-R basin (shadings; Figure 5c). This anomalous moisture flux convergence results from cyclonic circulation in the midlatitudes and anticyclonic circulation in the tropics.

The northerly wind anomalies to the western boundary of the cyclonic circulation and the southwesterly wind anomalies to the northwestern boundary of the anticyclonic circulation bring water vapor from the northwest North Pacific and Indian Ocean (vectors; Figure 5c), respectively. As a result, moisture fluxes converge over the YH-R basin. Compared with the distribution of SST anomalies during 1951–1986 (Figure 4c), warmer SSTs extended northeastward in the warm pool area during 1987–2018 (Figure 4d), which is consistent with the enlargement in the IPWP (Figure 4a,b). These changes in the SST anomalies are in agreement with the findings of previous studies [50], which found an obvious increase in summer SST over the WNP in the late 1980s. Concurrent with the extension of the warm pool, the anomalous convective heating extends northeastward, causing a northeastward movement of the anomalous relative vorticity pattern (Figure 5b) by exciting the Rossby wave train and a northeastward movement of the anomalous moisture fluxes (Figure 5d).

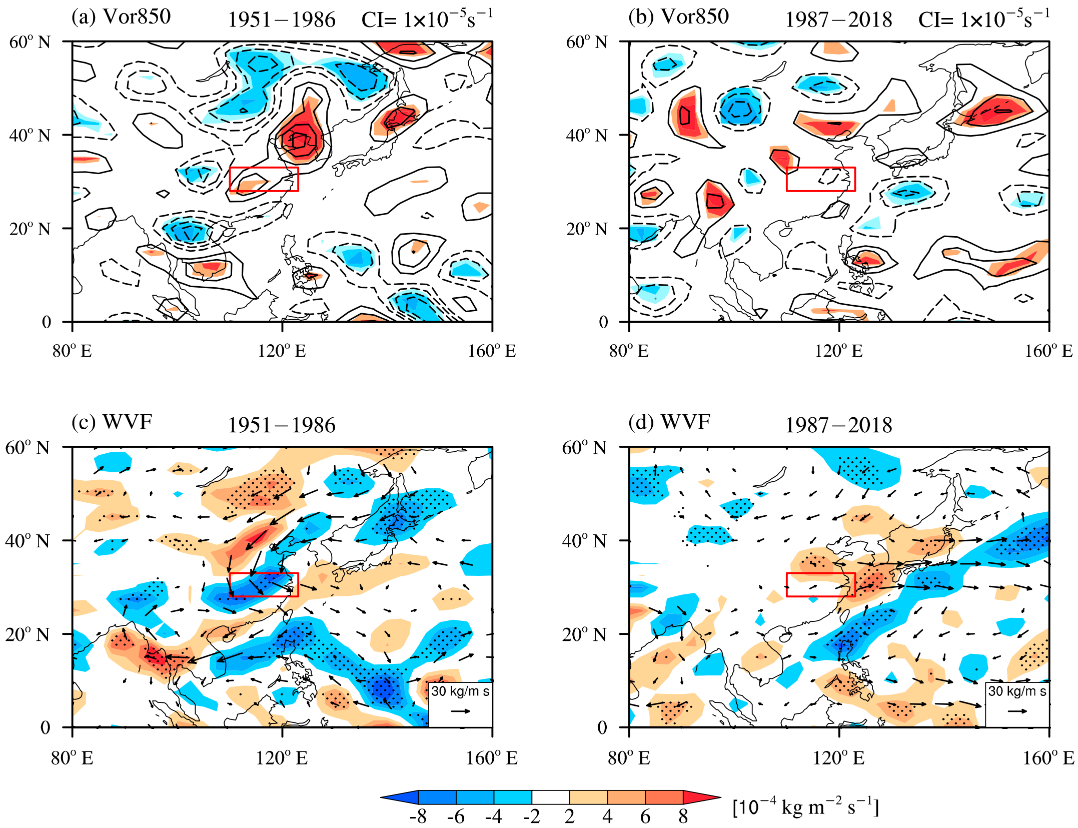

Figure 5. Regression maps of (**a**,**b**) relative vorticity (contour; unit: s^{-1}) at 850 hPa with respect to the normalized IPWP index for 1951–1986 and 1987–2018, respectively. (**c**,**d**) Same as for (**a**,**b**) but for the water vapor flux integration of 1000–300 hPa (vector; unit: kg m^{-1} s^{-1}) and its divergence (shading; unit: 10^{-4} kg m^{-2} s^{-1}). In (a–d), positive (negative) values are indicated by solid (dashed) contours with the zero contour omitted. The three orange (blue) shadings from shallow to deep in (**a**,**b**) indicate that positive (negative) anomalies are significant at the 90%, 95%, and 99% confidence levels based on a two-tailed Student's t test, respectively. The dotted regions in (**c**,**d**) indicate the 90% confidence level based on Student's t test. The red boxes indicate the YH-R basin.

The above analysis indicates a reduced connection between the EAP teleconnection pattern and the size variation in the IPWP. Figure 6 shows the correlation coefficients for a sliding 23-year moving window between the EAP index and the IPWP size index. The result confirms the decreased relationship between the EAP pattern and the size variation in the IPWP in the late 1980s. Therefore, the extension in the size of the IPWP induces a northeastward shift in the EAP pattern after the late 1980s by modulating the corresponding anomalous SST and convective activities. This northeastward shift in the

EAP teleconnection pattern gives rise to a weakened connection with summer rainfall anomalies over the YH-R basin.

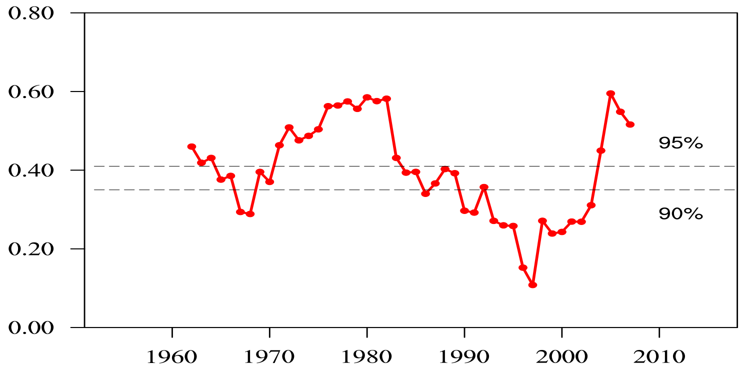

Figure 6. Time series of the running correlation with a 23-year window between the EAP index (multiplied by −1.0) and the normalized IPWP index during 1951–2018.

4. Discussion

This study mainly focused on the change in the size of the IPWP and its impacts on the northeastward shift in the Japanese action center of the EAP teleconnection pattern. Because the magnitude of the regressed anomalous circulation with respect to the IPWP index is smaller than that of the EAP index, there might be other factors responsible for the changes in the circulation related to the EAP teleconnection. In addition to local SST anomalies over the IPWP, previous studies have suggested that the EAP pattern can also be remotely driven by SST anomalies [51–53], such as the El Niño-Southern Oscillation (ENSO) events. Other studies have regarded the EAP pattern as an internal atmospheric dynamical mode embedded in the basic flow over East Asia [19,54]. A decadal change in the background circulation over East Asia in the late 1980s has been demonstrated [50]. Whether the northeastward shift in the Japanese action center of the EAP pattern is related to the change in the basic flow or the SST anomalies in remote regions needs further investigation but is beyond the scope of this study.

The present study revealed an evident weakened relationship between the EAP teleconnection pattern and summer rainfall in the YH-R valley from the late 1980s to the 2010s. Some previous studies noted that the summer rainfall over the middle-lower reaches of the Yangtze River has experienced a notable increase since the late 1970s [55–57]. Other factors play prominent roles in this interdecadal shift in summer rainfall over the Yangtze River basin, such as the extratropical west–east oriented Silk Road teleconnection pattern [58,59] or the WPSH [35]. Therefore, it is important to consider the influences of different factors to better understand the summer rainfall changes in the YH-R basin over eastern China.

5. Conclusions

The relationship between the interannual variations in YH-R valley summer rainfall and the EAP teleconnection pattern experienced an obvious interdecadal shift in the late 1980s. Before the late 1980s, the summer rainfall in the YH-R valley tended to be less than normal during positive EAP years, whereas after the late 1980s, the rainfall–EAP pattern connection became weaker and less evident. The present analysis reveals that the weakening relationship between the EAP pattern and the YH-R basin summer rainfall resulted from the notable northeastward displacement of the Japanese action center of the EAP pattern after the late 1980s. The vorticity anomalies regressed against the EAP index demonstrate that the positions of the Japanese action center of the EAP pattern were distinctly different during T1 and T2. Compared with the first subperiod, in which the Japanese action center was located along the conventional Meiyu band stretching from the YH-R valley to the area south of Japan, this action center had an obvious northeastward shift in the second subperiod, with vorticity anomalies confined around Japan. Concurrent with the northeastward shift in the Japanese action center, the negative phases of the EAP-associated anomalous vertical motion and moisture transport showed similar changes, which directly led to anomalous rainfall patterns. There was evident anomalous ascending motion and moisture flux convergence over the YH-R basin before the late 1980s. In contrast, after the late 1980s, the anomalous ascending motion and convergence of moisture transport over the YH-R basin obviously became weaker, which was detrimental to the emergence of anomalous positive summer rainfall there. Therefore, the anomalous vertical movement and water vapor transportation related to the northeastward-shifted Japanese action center of the EAP pattern in the late 1980s contributed to the notable weakening relationship between the summer rainfall anomalies in the YH-R basin and the EAP pattern.

The northeastward displacement of the Japanese action center is likely attributed to the interdecadal eastward expansion in the size of the IPWP after the late 1980s. Previous studies suggest that the EAP pattern is mainly triggered by anomalous convective activity over the Philippines that is related to the thermal state of the warm pool [9]. However, the detailed distribution of the convection and the motivated wave train teleconnection are different in the two subperiods due to the expansion of the IPWP. After the late 1980s, the area of the IPWP enlarged northeastward. Accordingly, anomalous convective heating extended northeastward, causing a northeastward movement of the anomalous relative vorticity pattern by exciting the Rossby wave train [3]. Thus, this finding suggests that the northeastward displacement of the Japanese action center of the EAP pattern can be explained to some extent by the northeastward extension of the IPWP in the late 1980s.

Author Contributions: Conceptualization, L.-T.Z. and J.H.; writing—original draft preparation, X.Y.; writing—review and editing, L.-T.Z. and J.H.; visualization, X.Y.; supervision, L.-T.Z. and J.H. All authors have read and agreed to the published version of the manuscript.

Funding: This study was funded by the National Key Research and Development Program of China (2016YFA0600603) and the Key Program of the Chinese Academy of Sciences (Grant QYZDY-SSW-DQC024).

Institutional Review Board Statement: Not applicable.

Informed Consent Statement: Not applicable.

Data Availability Statement: The monthly mean rainfall data from 160 stations were derived from the China Meteorological Administration operational network and are available upon request. Publicly available datasets were analyzed in this study. The NOAA PREC data can be found here: [https://psl.noaa.gov/data/gridded/data.prec.html] (accessed on 29 May 2021). The NCEP/NCAR reanalysis data can be found here: [https://psl.noaa.gov/data/gridded/data.ncep.reanalysis.html] (accessed on 29 May 2021). The ERSST.v3b data can be found here: [https://psl.noaa.gov/data/gridded/data.noaa.ersst.html] (accessed on 29 May 2021).

Conflicts of Interest: The authors declare no conflict of interest.

References

1. Huang, R.; Zhou, L. Research on the characteristics, formation mechanism and prediction of severe climatic disasters in China. *J. Nat. Disasters* **2002**, *11*, 1–9.
2. Zong, Y.Q.; Chen, X.Q. The 1998 flood on the Yangtze, China. *Natl. Hazards* **2000**, *22*, 165–184. [CrossRef]
3. Huang, R.H.; Li, W.J. Influence of the heat source anomaly over the western tropical Pacific on the subtropical high over East Asia. *Proc. Int. Conf. Gen. Circ. East Asia* **1987**, 40–51.
4. Lu, R.Y. Associations among the components of the east Asian summer monsoon system in the meridional direction. *J. Meteorol. Soc. Jpn.* **2004**, *82*, 155–165. [CrossRef]
5. Lin, Z.D.; Lu, R.Y. Interannual meridional displacement of the east Asian upper-tropospheric jet stream in summer. *Adv. Atmos. Sci.* **2005**, *22*, 199–211.
6. Sun, X.; Greatbatch, R.J.; Park, W.; Latif, M. Two major modes of variability of the East Asian summer monsoon. *Q. J. R. Meteorol. Soc.* **2010**, *136*, 829–841. [CrossRef]
7. Zhou, W.; Chan, J.C.L. Intraseasonal oscillations and the South China Sea summer monsoon onset. *Int. J. Clim.* **2005**, *25*, 1585–1609. [CrossRef]

8. Zhou, W.; Chan, J.C.L. ENSO and the South China Sea summer monsoon onset. *Int. J. Clim.* **2007**, *27*, 157–167. [CrossRef]
9. Nitta, T. Convective activities in the tropical western Pacific and their impact on the Northern Hemisphere summer circulation. *J. Meteorol. Soc. Jpn.* **1987**, *65*, 373–390. [CrossRef]
10. Huang, G. An index measuring the interannual variation of the East Asian summer monsoon—The EAP index. *Adv. Atmos. Sci.* **2004**, *21*, 41–52. [CrossRef]
11. Kosaka, Y.; Nakamura, H. Dominant mode of climate variability, intermodel diversity, and projected future changes over the summertime western North Pacific simulated in the CMIP3 models. *J. Clim.* **2011**, *24*, 3935–3955. [CrossRef]
12. Chen, Y.; Zhai, P.M. Synoptic-scale precursors of the East Asia/Pacific teleconnection pattern responsible for persistent extreme precipitation in the Yangtze River Valley. *Q. J. R. Meteorol. Soc.* **2015**, *141*, 1389–1403. [CrossRef]
13. Li, L.; Zhai, P.M.; Chen, Y.; Ni, Y.Q. Low-frequency oscillations of the East Asia-Pacific teleconnection pattern and their impacts on persistent heavy precipitation in the Yangtze-Huai River valley. *J. Meteorol. Res.* **2016**, *30*, 459–471. [CrossRef]
14. Sun, X.G.; Xu, Y.M.; Zhang, Z.Q.; Yang, X.Q. The tropical and extratropical-origin summer meridional teleconnections over East Asia. *Clim. Dyn.* **2019**, *53*, 721–735. [CrossRef]
15. Shang, W.; Li, S.S.; Ren, X.J.; Duan, K.Q. Event-based extreme precipitation in Central-Eastern China: Large-scale anomalies and teleconnections. *Clim. Dyn.* **2020**, *54*, 2347–2360. [CrossRef]
16. Lee, D.Y.; Ahn, J.B.; Yoo, J.H. Enhancement of seasonal prediction of East Asian summer rainfall related to western tropical Pacific convection. *Clim. Dyn.* **2015**, *45*, 1025–1042. [CrossRef]
17. Huang, R.H.; Sun, F.Y. Impacts of the tropical western Pacific on the East-Asian summer monsoon. *J. Meteorol. Soc. Jpn.* **1992**, *70*, 243–256. [CrossRef]
18. Wakabayashi, S.; Kawamura, R. Extraction of major teleconnection patterns possibly associated with the anomalous summer climate in Japan. *J. Meteorol. Soc. Jpn.* **2004**, *82*, 1577–1588. [CrossRef]
19. Kosaka, Y.; Nakamura, H. Structure and dynamics of the summertime Pacific-Japan teleconnection pattern. *Q. J. R. Meteorol. Soc.* **2006**, *132*, 2009–2030. [CrossRef]
20. Kosaka, Y.; Nakamura, H. Mechanisms of meridional teleconnection observed between a summer monsoon system and a subtropical anticyclone. Part II: A global survey. *J. Clim.* **2010**, *23*, 5109–5125. [CrossRef]
21. Kosaka, Y.; Xie, S.-P.; Lau, N.-C.; Vecchi, G.A. Origin of seasonal predictability for summer climate over the Northwestern Pacific. *Proc. Natl. Acad. Sci. USA* **2013**, *110*, 7574–7579. [CrossRef]
22. Song, J.; Li, C.Y. Contrasting relationship between tropical western North Pacific convection and rainfall over East Asia during Indian Ocean warm and cold summers. *J. Clim.* **2014**, *27*, 2562–2576. [CrossRef]
23. Li, X.Y.; Lu, R.Y. Extratropical factors affecting the variability in summer precipitation over the Yangtze River basin, China. *J. Clim.* **2017**, *30*, 8357–8374. [CrossRef]
24. Gong, H.; Wang, L.; Chen, W.; Wu, R.; Huang, G.; Nath, D. Diversity of the Pacific-Japan pattern among CMIP5 models: Role of SST anomalies and atmospheric mean flow. *J. Clim.* **2018**, *31*, 6857–6877. [CrossRef]
25. Lu, R. Interannual variability of the summertime North Pacific subtropical high and its relation to atmospheric convection over the warm pool. *J. Meteorol. Soc. Jpn.* **2001**, *79*, 771–783. [CrossRef]
26. Wang, B.; Wu, R.G.; Lau, K.M. Interannual variability of the Asian summer monsoon: Contrasts between the Indian and the western North Pacific-east Asian monsoons. *J. Clim.* **2001**, *14*, 4073–4090. [CrossRef]
27. Zhou, T.J.; Yu, R.C. Atmospheric water vapor transport associated with typical anomalous summer rainfall patterns in China. *J. Geophys. Res.* **2005**, *110*, 110. [CrossRef]
28. Hoskins, B.J.; Karoly, D.J. The steady linear response of a spherical atmosphere to thermal and orographic forcing. *J. Atmos. Sci.* **1981**, *38*, 1179–1196. [CrossRef]
29. Kurihara, K.; Tsuyuki, T. Development of the barotropic high around Japan and its association with Rossby wave-like propagations over the North Pacific: Analysis of August 1984. *J. Meteorol. Soc. Jpn.* **1987**, *65*, 237–246. [CrossRef]
30. Tao, L.; Li, T.; Ke, Y.-H.; Zhao, J.-W. Causes of interannual and interdecadal variations of the summertime Pacific-Japan-like pattern over East Asia. *J. Clim.* **2017**, *30*, 8845–8864. [CrossRef]
31. Huang, R.H.; Lu, L. Numerical simulation of the relationship between the anomaly of subtropical high over East Asia and the convective activities in the western tropical pacific. *Adv. Atmos. Sci.* **1989**, *6*, 202–214.
32. Zhou, L. Interdecadal variability in large and small warm pools in Western Pacific and their association with rainfall anomalies. *Atmos. Ocean. Sci. Lett.* **2014**, *7*, 56–61.
33. Yin, X.; Zhou, L.-T. Strengthened relationships of Northwest China wintertime precipitation with ENSO and midlatitude North Atlantic SST since the Mid-1990s. *J. Clim.* **2020**, *33*, 3967–3988. [CrossRef]
34. Ding, Y.; Wang, Z.; Sun, Y. Inter-decadal variation of the summer precipitation in East China and its association with decreasing Asian summer monsoon. Part I: Observed evidences. *Int. J. Clim.* **2008**, *28*, 1139–1161. [CrossRef]
35. Zhou, T.J.; Yu, R.C.; Zhang, J.; Drange, H.; Cassou, C.; Deser, C.; Hodson, D.L.R.; Sanchez-Gomez, E.; Li, J.; Keenlyside, N.; et al. Why the Western Pacific subtropical high has extended westward since the late 1970s. *J. Clim.* **2009**, *22*, 2199–2215. [CrossRef]
36. McPhaden, M.J.; Lee, T.; McClurg, D. El Niño and its relationship to changing background conditions in the tropical Pacific Ocean. *Geophys. Res. Lett.* **2011**, 38. [CrossRef]
37. Chung, P.-H.; Li, T. Interdecadal relationship between the mean state and El Niño types. *J. Clim.* **2013**, *26*, 361–379. [CrossRef]

38. Huangfu, J.; Huang, R.H.; Chen, W. Influence of tropical western Pacific warm pool thermal state on the interdecadal change of the onset of the South China Sea summer monsoon in the late-1990s. *Atmos. Ocean. Sci. Lett.* **2015**, *8*, 95–99.
39. Wang, L.; Huang, G.; Chen, W.; Zhou, W.; Wang, W. Wet-to-dry shift over Southwest China in 1994 tied to the warming of tropical warm pool. *Clim. Dyn.* **2018**, *51*, 3111–3123. [CrossRef]
40. Wu, R.G.; Yang, S.; Wen, Z.P.; Huang, G.; Hu, K.M. Interdecadal change in the relationship of southern China summer rainfall with tropical Indo-Pacific SST. *Appl. Clim.* **2012**, *108*, 119–133. [CrossRef]
41. Chen, M.Y.; Xie, P.P.; Janowiak, J.E.; Arkin, P.A. Global land precipitation: A 50-yr monthly analysis based on gauge observations. *J. Hydrometeorol.* **2002**, *3*, 249–266. [CrossRef]
42. Kalnay, E.; Kanamitsu, M.; Kistler, R.; Collins, W.; Deaven, D.; Gandin, L.; Iredell, M.; Saha, S.; White, G.; Woollen, J.; et al. The NCEP/NCAR 40-year reanalysis project. *Bull. Amer. Meteorol. Soc.* **1996**, *77*, 437–471. [CrossRef]
43. Smith, T.M.; Reynolds, R.W.; Peterson, T.C.; Lawrimore, J. Improvements to NOAA's historical merged land-ocean surface temperature analysis (1880–2006). *J. Clim.* **2008**, *21*, 2283–2296. [CrossRef]
44. Kosaka, Y.; Xie, S.-P.; Nakamura, H. Dynamics of interannual variability in summer precipitation over East Asia. *J. Clim.* **2011**, *24*, 5435–5453. [CrossRef]
45. Huang, R.; Chen, J.; Wang, L.; Lin, Z. Characteristics, processes, and causes of the spatio-temporal variabilities of the East Asian monsoon system. *Adv. Atmos. Sci.* **2012**, *29*, 910–942. [CrossRef]
46. Takaya, K.; Nakamura, H. A formulation of a phase-independent wave-activity flux for stationary and migratory quasigeostrophic eddies on a zonally varying basic flow. *J. Atmos. Sci.* **2001**, *58*, 608–627. [CrossRef]
47. Xu, P.; Wang, L.; Chen, W.; Feng, J.; Liu, Y. Structural changes in the Pacific-Japan pattern in the late 1990s. *J. Clim.* **2019**, *32*, 607–621. [CrossRef]
48. Chen, X.L.; Zhou, T.J. Relative role of tropical SST forcing in the 1990s periodicity change of the Pacific-Japan pattern interannual variability. *J. Geophys. Res.* **2014**, *119*, 13043–13066. [CrossRef]
49. Yim, S.-Y.; Wang, B.; Kwon, M. Interdecadal change of the controlling mechanisms for East Asian early summer rainfall variation around the mid-1990s. *Clim. Dyn.* **2014**, *42*, 1325–1333. [CrossRef]
50. Zhang, R.H.; Wu, B.Y.; Zhao, P.; Han, J.P. The decadal shift of the summer climate in the late 1980s over eastern China and its possible causes. *Acta Meteorol. Sin.* **2008**, *22*, 435–445.
51. Wang, B.; Wu, R.G.; Fu, X.H. Pacific-East Asian teleconnection: How does ENSO affect East Asian climate? *J. Clim.* **2000**, *13*, 1517–1536. [CrossRef]
52. Xie, S.-P.; Hu, K.; Hafner, J.; Tokinaga, H.; Du, Y.; Huang, G.; Sampe, T. Indian Ocean capacitor effect on Indo-Western Pacific climate during the summer following El Niño. *J. Clim.* **2009**, *22*, 730–747. [CrossRef]
53. Xie, S.-P.; Kosaka, Y.; Du, Y.; Hu, K.; Chowdary, J.S.; Huang, G. Indo-western Pacific ocean capacitor and coherent climate anomalies in post-ENSO summer: A review. *Adv. Atmos. Sci.* **2016**, *33*, 411–432. [CrossRef]
54. Kosaka, Y.; Nakamura, H. Mechanisms of meridional teleconnection observed between a summer monsoon system and a subtropical anticyclone. Part I: The Pacific-Japan pattern. *J. Clim.* **2010**, *23*, 5085–5108. [CrossRef]
55. Gong, D.-Y.; Ho, C.-H. Shift in the summer rainfall over the Yangtze River valley in the late 1970s. *Geophys. Res. Lett.* **2002**, *29*, 78-1. [CrossRef]
56. Hu, Z.Z.; Yang, S.; Wu, R.G. Long-term climate variations in China and global warming signals. *J. Geophy. Res.* **2003**, 108. [CrossRef]
57. Yu, R.; Zhou, T. Seasonality and three-dimensional structure of interdecadal change in the East Asian monsoon. *J. Clim.* **2007**, *20*, 5344–5355. [CrossRef]
58. Enomoto, T.; Hoskins, B.J.; Matsuda, Y. The formation mechanism of the Bonin high in August. *Q. J. R. Meteorol. Soc.* **2003**, *129*, 157–178. [CrossRef]
59. Yasui, S.; Watanabe, M. Forcing processes of the summertime circumglobal teleconnection pattern in a dry AGCM. *J. Clim.* **2010**, *23*, 2093–2114. [CrossRef]